MAGNETICALLY LEVITATED CENTRIFUGAL BLOOD PUMP WITH RADIALLY SUSPENDED SELF-BEARING MOTOR

Hiroyuki Onuma
Department of Mechanical Engineering, Ibaraki University, Hitachi, Ibaraki 316-8511, Japan
honuma@mech.ibaraki.ac.jp
Toru masuzawa, Ken-ichi Matsuda, and Yohji Okada
Department of Mechanical Engineering, Ibaraki University, Hitachi, Ibaraki 316-8511, Japan
masuzawa@mech.ibaraki.ac.jp, matsu@mech.ibaraki.ac.jp, and okada@mech.ibaraki.ac.jp

ABSTRACT

We have developed a magnetically levitated centrifugal blood pump with a radially suspended self-bearing motor. In this study, the self-bearing motor was improved to enhance its levitation and pump performance toward practical usage. Two and three-dimensional magnetic field analyses based on the finite element method were performed to improve the self-bearing motor. Material of the rotor was also changed from magnetic stainless steel to laminated silicon steel to reduce the power loss. The maximum rotational speed, the maximum flow rate and the maximum head pressure of the maglev pump were increased upto 2400 rpm, 9.7 l/min and 313 mmHg, respectively. The maximum oscillating amplitude of the levitated impeller decreased from 0.16 mm to 0.06 mm. The maglev centrifugal blood pump has the potential to be an artificial heart for next generation.

INTRODUCTION

Magnetically levitated centrifugal blood pump has been developed for an implantable artificial heart. Major required point in development of the implantable artificial heart are high durability of the mechanism for implantation because the device should be driven in the patient's body for several years without any maintenance. Also, the device should be small and thin to implant. Thickness of the device is more important than width of it from the point of view anatomical fitting. The purpose of this study is to develop a durable centrifugal blood pump with a thin, small and high efficient actuator. The developed self-bearing motor actively suspends a rotor in the radial direction and rotates with electrical magnetic fields. Therefore, the pump has no mechanical parts such as seals and bearings of the motor, and has high durability. Developed prototype of a magnetically levitated centrifugal blood pump indicated that the maximum rotational speed of 2000 rpm, the maximum flow rate of 8.2 l/min, and the maximum pressure head of 220 mmHg [1][2]. The previous results proved the possibility of the magnetically levitated centrifugal pump as an implantable artificial heart. In this study, the self-bearing motor was improved to enhance its levitation performance and the pump performance of the device toward practical usage.

METHODS

Self-bearing motor

Figure 1 shows the radially suspended self-bearing motor. The outer rotor structure, that a rotor is set around a stator, is adopted to miniaturize the self-bearing motor. The rotor, which is a yoke itself, has four thin permanent magnets on inner circumferential surface. The thickness of the permanent magnets is 0.7 mm. The outer diameter, the inner diameter and the thickness of the rotor are 63.4 mm, 53.4 mm, and 8 mm, respectively. The stator has twelve radial poles. The pole has a bulge at the end faced on the rotor to distribute the magnetic field effectively and a narrow radial spoke to wind coil wire. The diameter and the thickness of the prototype stator are 50 mm, 8 mm, respectively. Rotation coils to produce 3-phase 4-pole magnetic field and levitation coils to produce 2-phase 6-pole magnetic field are constructed separately in the stator. The plus minus two-pole algorithm is adopted to levitate and rotate the rotor. Radial gap between the rotor and the stator

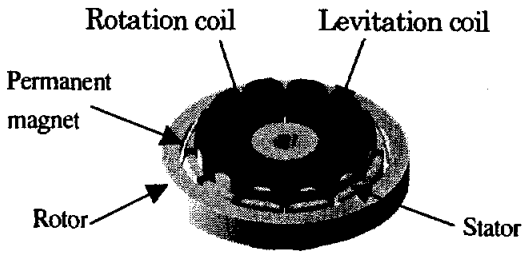

FIGURE 1: Radially suspended self-bearing motor

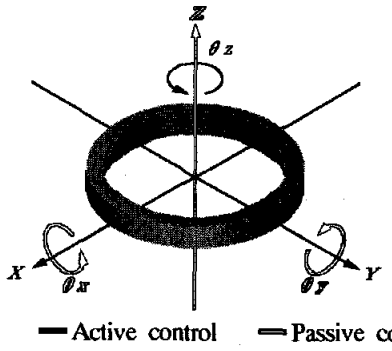

FIGURE 2:Control degrees of freedom of the levitated rotor

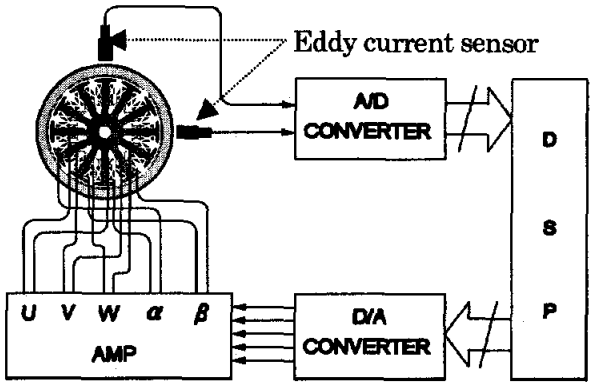

FIGURE 3: Schematic of control system

is set as 1 mm. Closed magnetic circuit was formed through the stator pole and the rotor yoke. Figure 2 shows the control degrees of freedom of the levitated rotor. Two radial degrees of freedom of the rotor and rotation of the rotor are controlled actively by electric magnets constructed on the stator. Axial movement and tilt of the rotor are restricted by passive stability based on thin rotor structure to simplify the control system. Figure 3 shows the schematics of control system. Levitation and rotation of the rotor were controlled numerically by using a digital signal processor. Two eddy current sensors are used to measure rotor radial position.

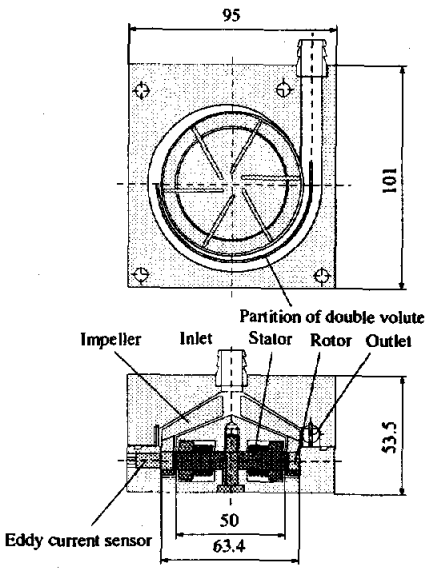

FIGURE 4: Magnetically levitated centrifugal pump

Magnetically levitated centrifugal pump

Figure 4 shows the magnetically levitated centrifugal pump with a radially suspended self-bearing motor. An impeller of the centrifugal pump with six open type vanes was set on the rotor. The centrifugal pump has a double volute in order to minimize the fluid dynamic imbalance inside the centrifugal pump.

Optimization of the self-bearing motor

Improvement of the stator. Three-dimensional and two-dimensional magnetic field analyses based on the finite element method with commercial software ANSYS were performed to change the design of the stator. Three-dimensional magnetic field analysis was used to determine location of the magnetic saturation of prototype motor and to confirm the effect of design changing on the magnetic saturation. Figure 5 shows the analysis models used for three-dimensional magnetic field analysis. The analysis models contain a stator part and a rotor part. The thickness of the stator was enlarged to twice of the prototype stator in a redesigned model. The size of the rotor in both models is same. The results of three-dimensional magnetic field indicated that the magnet saturation could be prevented with the thickened stator. But, the passive stability performance deteriorated with the changing of stator thickness because fringing field enlarged at the stator end faced on the rotor. To minimize the effect of the fringing field, the thickness of the stator bulge was kept to the same

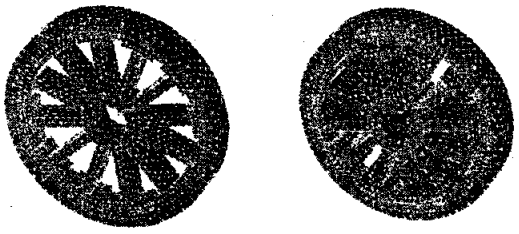

(a) Prototype motor (b) Redesigned motor

FIGURE 5: Three-dimensional analysis model

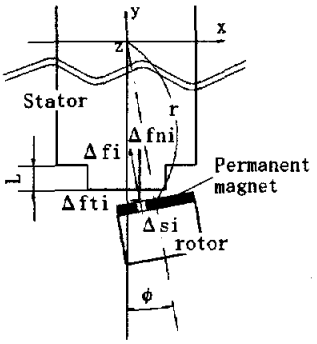

FIGURE 6: Schematic of two-dimensional analysis

thickness with the rotor. Proper radial length of the bulge thin part was estimated with two-dimensional magnetic field analysis [3]. Figure 6 shows schematic of two-dimensional analysis. The radial length L was changed from 0.5 mm to 5.0 mm in the analysis. Δfi denotes the attractive force for the small element Δsi of the permanent magnet divided into K segments in the x direction. Let Δfti and Δfni be the tangential and normal components of the attractive force Δfi acting on a small element Δsi of the rotor. When the rotor is tilted around the z axis, the tangential component Δfti gives the restoring torque τz. This torque is asymmetric with respect to the z axis and can be written as

$$\tau z = \int_x \Delta \tau z = \sum_{i=1}^{K} \left(r |\cos \phi| \Delta fti + x \Delta fni \right)$$

The change of restoring torque τz by changing the radial length L was evaluated in the analysis.

Change of the rotor material. Material of the rotor was changed from magnetic stainless steel to laminated silicon steel to reduce the power loss inside the rotor. The rotor was constructed with 23 sheets of silicon steel 0.35 mm thick.

EXPERIMENTS

The effectiveness of the stator thickness change was evaluated to measure the magnetic flux density and the attractive force. The magnetic flux density between the stator and the rotor was measured with a magnetic flux probe. The attractive force in the radial direction was measured directly with a strain gage sensor to evaluate control performance in the radial direction. The attractive force in axial direction and restoring torque were directly measured with a strain gage sensor to evaluate passive stability performance of the motor.

The motor performance was measured to evaluate the effectiveness of the rotor material change and the stator redesign. The rotor was attached to a connection shaft of torque meter. The torque and electrical input power to the motor was measured by using a digital torque meter and a power meter. In this experiment, the motor coils were only excited. The following three motors were examined. 'A'motor consists of the prototype stator and the rotor made of magnetic stainless steel. 'B'motor consists of the prototype stator and the rotor made of laminated silicon steel. 'C'motor consists of the improved stator and the rotor made of laminated silicon steel.

Finally, the magnetically levitated centrifugal pump was constructed with the improved motor. The centrifugal pump was connected to a closed mock circuit filled with the water, and magnetic levitation performance and pump performance were examined.

RESULTS

Magnetic field analysis

The estimated flux densities in the gap between the rotor and stator and in the spokes of poles were shown in Table 1. The maximum flux density was observed in the spokes. The prototype stator had magnetic saturation located at spokes of poles. The magnetic saturation was prevented successfully by enlarging the cross-sectional area of the spokes in the redesigned stator increased thickness. The flux density in the gap between the rotor and stator also increased.

The estimated restoring torque was shown in Figure 7. The restoring torque decreased in cases with shorter radial length of the bulge thin part than 2.5 mm. Therefore, the length of the thin part was determined as 2.5 mm. The improved stator is shown in Figure 8

TABLE 1: Estimated flux density

	Gap	Spokes
Prototype motor	0.45 [T]	2.67 [T]
Redesigned motor	0.58 [T]	1.44 [T]

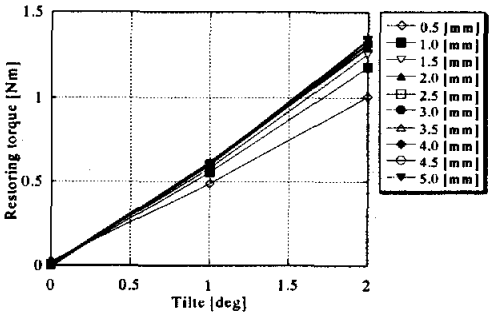

FIGURE 7: Estimated restoring torque

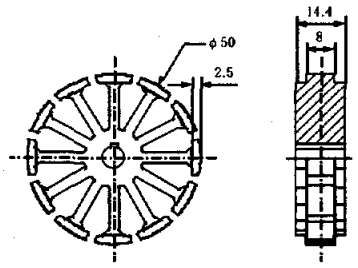

FIGURE 8: Improved stator

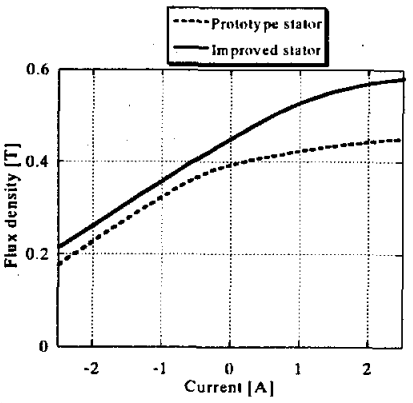

FIGURE 9: Flux density

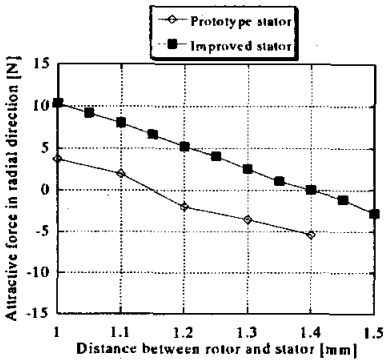

FIGURE 10: Attractive force in radial direction

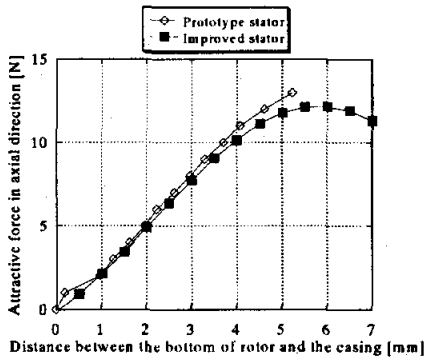

FIGURE 11: Attractive force in axial direction

Saturation of flux density

The magnetic flux density measured in the gap is shown in Figure 9. Magnetic saturation occurred when the flux density is over 0.4 T with the prototype stator. Magnetic saturation was prevented and the maximum magnetic flux density increased from 0.45 T to 0.6 T by using the improved stator. In the range of -1 A to 1 A of levitation control current good linearity between the current and the flux density was realized.

Attractive force and restoring torque

Measured attractive force in the radial direction is shown in Figure 10. The maximum attractive force in radial direction increased from 5 N to 15 N with the improved stator. The controllable displacement of rotor was expanded to 0.4 mm from 0.2 mm. Measured attractive force in the axial direction and measured restoring torque are shown in Figure 11 and 12. The axial attraction and restoring torque were not change with the stator redesign. The passive stability performance of improved stator is similar to that of prototype stator.

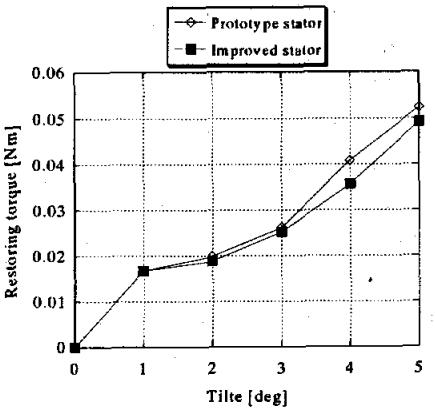

FIGURE 12: Restoring torque

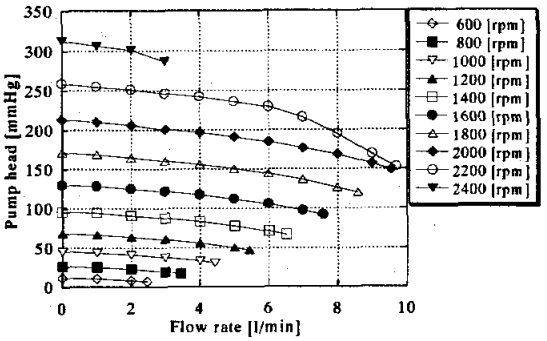

FIGURE 14: HQ characteristics

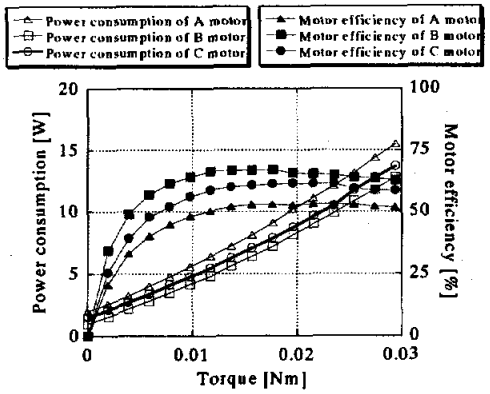

FIGURE 13: Relationship between power consumption and torque and relationship between motor efficiency and torque

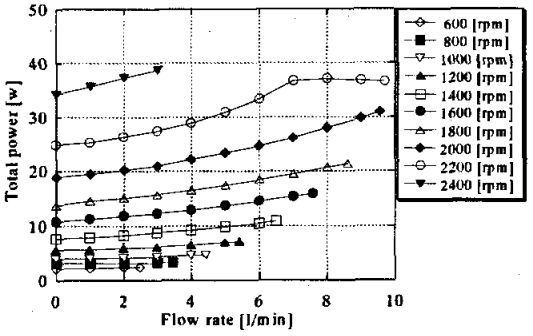

FIGURE 15: Total power consumption

Motor performance

The relationship between the motor efficiency, and the power consumption, and the torque is shown in Figure 13. The maximum motor efficiency of 'A'motor, 'B'motor and 'C'motor were 54 %, 67 % and 61 %, respectively. The power consumption of B motor with the laminated silicon steel rotor decreased by about 3 W compared with 'A'motor which is the prototype motor. The motor performance improved by using the rotor made of laminated silicon steel. The power consumption of 'C'motor with the thickened stator and the laminated silicon steel rotor increased by about 1 W compared with 'B'motor. But, the power consumption of 'C'motor decreased by about 2 W compared with 'A'motor.

Pump performance

The pump performance, the total power consumption and the total efficiency of the maglev pump are shown in Figure 14, Figure 15 and Figure 16, respectively. The levitated rotor could be rotated up to a rotational speed of 2400 rpm with pumping. The maximum flow rate and the maximum head pressure were increased to 9.7 l/min and 313 mmHg, respectively. The maximum total efficiency was 11 %. The input electric power and pump efficiency with a pressure head of 100 mmHg and a flow rate of 5 l/min were 12 W and 9 %.

Position control ability

The change in oscillation amplitude of the levitated rotor during pumping due to increasing the rotating speed is shown in Figure 17. The maximum oscillating amplitude in radial direction during pumping the water decreased from 0.16 mm to 0.06 mm by improving the self-bearing motor.

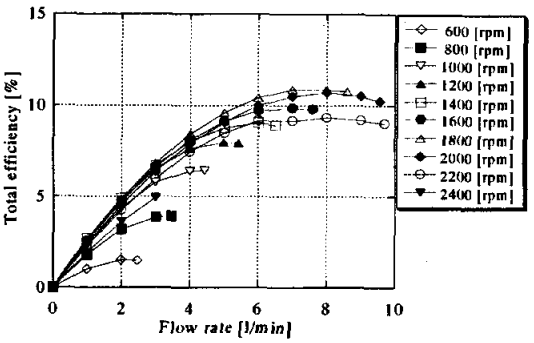

FIGURE 16: Total efficiency

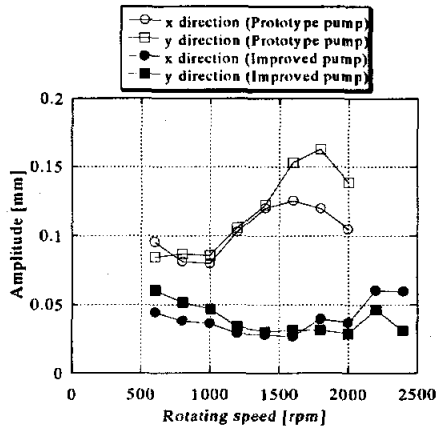

FIGURE 17: Maximum oscillating amplitude in radial direction

DISCUSSION

The reason that the magnetic saturation was located at the spokes of the poles in the prototype stator is as follows. The cross-sectional area in the poles decreases at the boundary between the spoke and the bulge, and the magnetic flux concentrated in the spokes. The magnetic saturation was prevented successfully by enlarging the cross-sectional area of the spokes in the improved stator increased thickness. The flux change linearity and the attractive force in radial direction were improved by the thickened stator. The declines of the restoring torque of the thickened stator were avoided by making the thin circumference part at the bulge. The passive stability of the thickened stator was maintained similar with that of the prototype stator.

The motor performance improved by using the rotor made of laminated silicon steel. This reason of it was that the eddy current losses and the hysteresis losses inside rotor were decreased by using laminated silicon steel. The motor performance deteriorated little by using the thickened stator because the copper losses of the coil increased since the coil length increased in the thickened stator. However, the motor performance with the thickened stator and the laminated silicon steel rotor is better than that of the prototype motor.

The oscillation amplitude in the radial direction was decreased drastically from 0.16 mm to 0.04 mm. The impeller of the maglev pump rotated without touching a casing during pumping. The sufficient pump performance of the magnetically levitated centrifugal blood pump with self-bearing motor was confirmed. We consider the self-bearing motor has enough efficiency for the artificial heart. The levitated centrifugal pump with the self-bearing motor has sufficient performance as an implantable artificial heart.

CONCLUSION

The self-bearing motor was redesigned to prevent magnetic saturation and to improve the motor performance. The magnetic flux density in the gap and the attraction were increased and the performance of the self-bearing motor was improved successfully. The pump performance was also improved. The magnetically levitated centrifugal blood pump with radially suspended self-bearing motor has the potential to be an artificial heart for next generation.

REFARENCE

1. Toru Masuzawa, Toshiyuki Kita, Ken-ichi Matsuda, Seung-Jong Kim, and Yohji Okada, Outer Rotor Type Self-Bearing Motor for an Artificial Heart. The fifth international conference on Motion and Vibration Control, 2000; 393-396
2. Toru Masuzawa, Toshiyuki Kita, and Yohji Okada, An Ultradurable and Compact Rotary Blood Pump with a Magnetically Suspended Impeller in the Radial Direction. Artificial Organs, 2001; 25(5): 395-399
3. Ken-ichi Matsuda, Toshiyuki Kita, Yohji Okada, Toru Masuzawa, Tetsuo Ohishi, Yoshiyuki Taenaka, and Takashi Yamane, Radial-type Self-Bearing Motor for Nonpulsatile-Tyoe Artificial Heart. JSME International Journal, 2000; Series C, Vol.43, No.4